

# Lawrence Berkeley National Laboratory

## Recent Work

### Title

EVIDENCE FOR THE GROWTH MECHANISM OF Cr<sub>2</sub>O<sub>3</sub> AT LOW OXYGEN POTENTIALS

### Permalink

<https://escholarship.org/uc/item/0171b4mk>

### Authors

Hindam, H.  
Whittle, D.P.

### Publication Date

1982-07-01



# Lawrence Berkeley Laboratory

UNIVERSITY OF CALIFORNIA

RECEIVED  
LAWRENCE  
BERKELEY LABORATORY

SEP 30 1982

LIBRARY AND  
DOCUMENTS SECTION

## Materials & Molecular Research Division

Submitted to the Journal of the Electrochemical  
Society

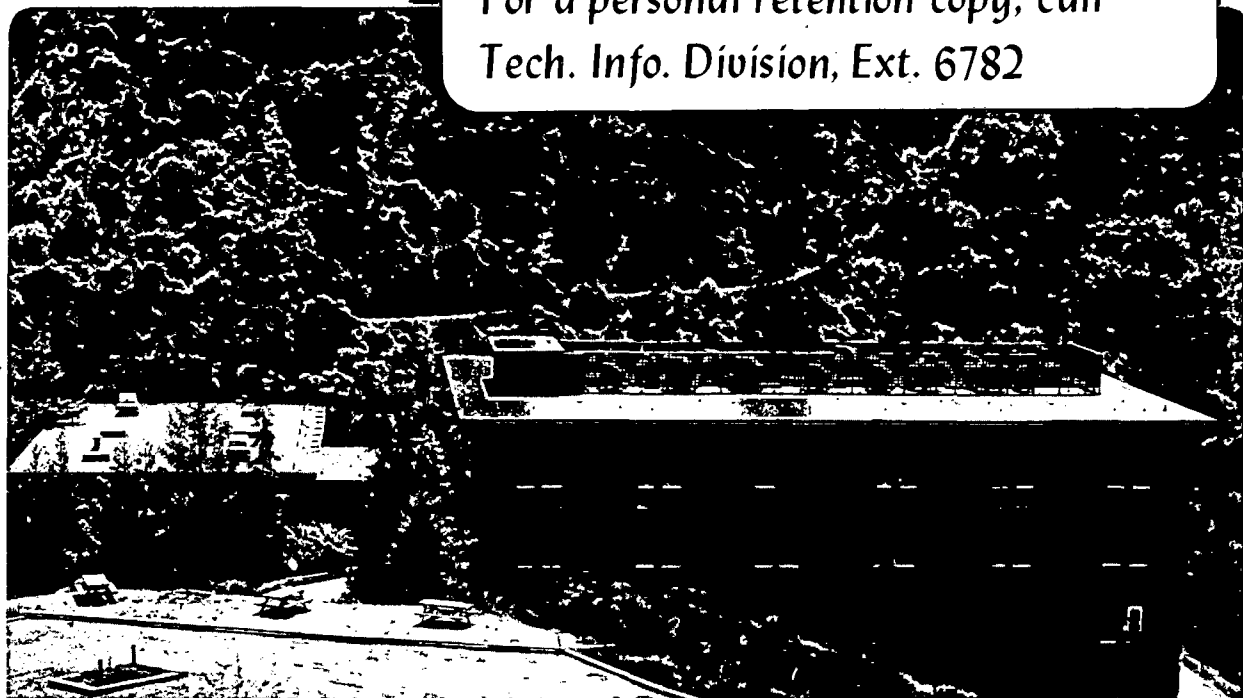
EVIDENCE FOR THE GROWTH MECHANISM OF  $Cr_2O_3$  AT  
LOW OXYGEN POTENTIALS

H. Hindam and D.P. Whittle

July 1982

TWO-WEEK LOAN COPY

*This is a Library Circulating Copy  
which may be borrowed for two weeks.  
For a personal retention copy, call  
Tech. Info. Division, Ext. 6782*



LBL-14834  
c. 2

## DISCLAIMER

This document was prepared as an account of work sponsored by the United States Government. While this document is believed to contain correct information, neither the United States Government nor any agency thereof, nor the Regents of the University of California, nor any of their employees, makes any warranty, express or implied, or assumes any legal responsibility for the accuracy, completeness, or usefulness of any information, apparatus, product, or process disclosed, or represents that its use would not infringe privately owned rights. Reference herein to any specific commercial product, process, or service by its trade name, trademark, manufacturer, or otherwise, does not necessarily constitute or imply its endorsement, recommendation, or favoring by the United States Government or any agency thereof, or the Regents of the University of California. The views and opinions of authors expressed herein do not necessarily state or reflect those of the United States Government or any agency thereof or the Regents of the University of California.

# EVIDENCE FOR THE GROWTH MECHANISM OF $\text{Cr}_2\text{O}_3$ AT LOW OXYGEN POTENTIALS<sup>+</sup>

H. Hindam<sup>x</sup> and D. P. Whittle<sup>o</sup>

Materials and Molecular Research Division  
Lawrence Berkeley Laboratory  
<sup>o</sup>and Department of Materials Science and Mineral Engineering  
University of California  
Berkeley, California 94720

## ABSTRACT

The growth rate of  $\text{Cr}_2\text{O}_3$  on pure Cr, Ni-25 and 50% Cr and Co-25% Cr in flowing  $\text{CO-CO}_2$  mixtures of effective oxygen pressures in the range  $8.4 \times 10^{-15}$  to  $8.3 \times 10^{-9}$  atm. at  $1000^\circ\text{C}$  has been measured. The parabolic growth constant is virtually independent of oxygen potential for both pure Cr and the alloys; for the alloys it is about an order of magnitude smaller than for pure Cr. These results provide supportive evidence for Cr interstitials being the predominating mobile defect species in  $\text{Cr}_2\text{O}_3$  under these conditions.

## INTRODUCTION

$\text{Cr}_2\text{O}_3$  is an important oxide: it provides the protective scale on many technologically important alloys. Nevertheless, neither its defect and transport properties, nor its growth mechanism are well understood. This is the case in spite of the many investigations of  $\text{Cr}_2\text{O}_3$  formation on both pure Cr and many  $\text{Cr}_2\text{O}_3$ -forming alloys. Most of these have been summarized recently (1, 2).

With some justifiable reservations, the growth kinetics of  $\text{Cr}_2\text{O}_3$  are generally diffusion-controlled (parabolic), at least at some stage of the reaction. However, apparent rate constants at  $1000^\circ\text{C}$ , for example, can differ

---

<sup>+</sup>This work was supported by the Director, Office of Energy Research, Office of Basic Energy Sciences, Materials Sciences Division of the U.S. Department of Energy under Contract No. DE-AC03-76SF00098.

<sup>x</sup>Present Address: Physical Metallurgy Research Laboratory, CANMET, Ottawa, Ont., Canada K1A0G1; on leave to: Industrial Materials Research Institute, NRC, Bel-Air, Montreal, Que., Canada H4C2K3

by as much as a factor of  $10^4$ . Indeed, the largest scatter in rate constants is obtained with growth on pure Cr, rather than with alloys (2).

Considerable effort has been expended in attempts to explain these large differences, but little consensus has been achieved. Nevertheless, one of the major contributory factors is the development of non-uniform growth of the  $\text{Cr}_2\text{O}_3$  in the form of oxide nodules, blisters, convoluted and multi-layered scales: the detailed metallographic observations of several authors (1, 3, 4) provide excellent examples. Detachment of the  $\text{Cr}_2\text{O}_3$  scale from the substrate as a result of poor adhesion, or stress development during growth supposedly does not stifle its growth since the vapor pressure and transport rate of Cr from the metal to the underside of the oxide are high enough to sustain continued growth. Cracking of the detached oxide and formation of a second or more layer of  $\text{Cr}_2\text{O}_3$  is a common occurrence. There is seemingly little correlation with experimental variables, such as surface condition, sample purity, temperature, oxygen pressure, etc.

Nevertheless, although not definable a priori, under certain conditions,  $\text{Cr}_2\text{O}_3$  does grow as a protective layer which may or may not be adherent to the substrate, and it is possible to rationalize the parabolic growth constant by comparing its magnitude with that calculated from independent diffusion measurements of the transport rate of the predominantly mobile species in the oxide. In doing this, Lillerud and Kofstad (1) were only able to rationalize their results by assuming that the important cation lattice defects were Cr interstitials and not vacancies, as seems to have been commonly accepted in literature discussions, although the basis for this seems rather obscure, or at least tentative. Kröger (5) has comprehensively reviewed all the evidence and is unable to differentiate between  $V_{\text{Cr}}^{\alpha'}$  or  $\text{Cr}_i^{\alpha'}$  as the predominating defect.

An important implication of Cr interstitials being the predominant defects is that the parabolic growth constant is independent of oxygen pressure, as

observed (1), and that Cr diffusivity in  $\text{Cr}_2\text{O}_3$  increases with decreasing oxygen pressure. According to Lillerud and Kofstad (1), this explains the observation that the Cr diffusion coefficient was approximately 10 times higher in hot pressed than in sintered  $\text{Cr}_2\text{O}_3$  compacts (6). The original authors (6) reported that the hot pressed samples contained free Cr, suggesting (1) that the effective oxygen pressure within the samples was close to the  $\text{Cr}/\text{Cr}_2\text{O}_3$  dissociation pressure and lower than that existing within sintered samples which were annealed in nitrogen (residual oxygen being  $10^{-7}$  to  $10^{-6}$  atm.) As pointed out (1), enhanced sintering of  $\text{Cr}_2\text{O}_3$  as the oxygen partial pressure is decreased is also consistent with an n-type defect model, oxygen vacancies being the minority defect.

The present paper reports additional data which support the proposed (1) defect model. It is not meant to be a comprehensive study, but represents data obtained for the growth kinetics of  $\text{Cr}_2\text{O}_3$  on Cr and Cr-rich alloys as part of a research program on alloy behavior in sulfur-containing atmospheres of low oxygen potential (7).

## EXPERIMENTAL

Samples of pure Cr, NiCr and CoCr alloys were cut from induction melted and vacuum cast ingots to dimensions approximately 12x12x1 mm and their surfaces prepared by grinding through 600 grit SiC papers. After cleaning, the samples were suspended by quartz fiber in a Cahn 1000 microbalance assembly, for which, under the present operating conditions, the sensitivity of the thermogravimetric measurements was better than 30  $\mu\text{g}$ . The sample hung in the center of the inner of two concentric mullite tubes. These had diameters of approximately 1 and 2.5 cm. respectively. The gas flow passed down the outer tube and up the inner one, and so was preheated before coming into contact with the sample. The mullite tubes were heated by

a quartz lamp furnace, controllable within  $\pm 1^\circ\text{C}$ . A purified argon gas flow passed through the balance head chamber, and was exhausted with the reactive gas above the furnace tube.

Control of the reactive gas composition was achieved by mixing metered flows of certified grade  $\text{CO}_2$  and  $\text{CO}_2$ -CO mixtures. Prior to mixing, the flow rates of the individual supplies were controlled through motorized needle valves actuated through calibrated mass flow meters. The flow rate of the final gas mixture, corresponding to a linear velocity of 0.3 cm/sec, was also measured by a calibrated mass flow meter and was kept constant throughout all the experiments, with the exception of a few runs to determine the effect, if any, of this variable on the reaction rate.

The kinetic data were recorded on a chart recorder, the experimental data points marked on accompanying figures indicating the values taken from the original chart recordings.

Samples were examined after exposure by standard techniques.

## RESULTS

Figure 1 presents weight change data plotted as a function of square root of time for pure Cr exposed at  $1000^\circ\text{C}$  to a number of CO/CO<sub>2</sub> mixtures, as detailed in Table I; the effective oxygen partial pressure is also included. Protective behavior was always observed up to the maximum periods of exposure. All the lines deviate slightly from linearity; however, as discussed later, this is related to slight grain coarsening during scale growth and does not invalidate the determination of a meaningful parabolic rate constant. Indeed, linear correlation coefficients are always better than 0.999. The rate constants are included in Table I.

There is no systematic variation of the parabolic rate constants with oxygen partial pressure. The slight differences are almost certainly related

to subtle changes in the grain size of the  $\text{Cr}_2\text{O}_3$ , which may be dependent on the exposure conditions, although this was not studied in detail. For a particular set of conditions, the kinetic curves are reproducible. Figure 2 shows an example of three independent weight gain/time curves in  $\text{CO}_2$ -0.3 vol. % CO at  $1000^\circ\text{C}$ , at linear gas velocities of 0.03, 0.33 and 0.66 cm/sec. The weight changes at the longest exposure time (15 h) are within  $\pm 50 \mu\text{g}/\text{cm}^2$ : the standard deviation of the parabolic rate constants for the three runs is  $\pm 0.05 \times 10^{-10} \text{ g}^2 \text{ cm}^{-4} \text{ sec}^{-1}$ .

In addition, volatilization of  $\text{Cr}_2\text{O}_3$  to  $\text{CrO}_3(3)$  is not expected at these low oxygen pressures. This was confirmed by recording the weight change of a large flake of  $\text{Cr}_2\text{O}_3$  (scale spalled from one of the samples) exposed to the  $\text{CO}_2$ -0.1% CO mixture (highest  $P_{\text{O}_2}$ ). Within the sensitivity of the microbalance, no weight change was observed over a time period corresponding to that of a typical experiment.

In all cases only uniform, single layer scales of  $\text{Cr}_2\text{O}_3$  were ever observed, although in most cases these spalled from the surface as large rectangular flakes when cooled rapidly from the reaction temperature. They exhibited a macroscopic, wrinkled appearance, inferring plastic deformation without fracture at these reduced oxygen potentials. Presumably, they were not totally adherent to the substrate; however, they evidently did not crack open. Figure 3 shows a typical fracture section through spalled flake. Equiaxed grains with uniform, sub-micron size are evident, although not easily measurable. Some whiskers protrude out of the outer surface of the scale, but would not contribute any significant amount to the total weight gain.

Figure 4 shows weight change data for Co-25 wt.% Cr and Ni-25 and 50 wt.% Cr at  $1000^\circ\text{C}$  in different gas mixtures as detailed in Table II. Again, the rates are substantially parabolic, decreasing very slightly with extended exposure, but not sufficiently that a meaningful average parabolic rate



constant cannot be defined. The rates, given in Table II, are virtually independent of gas composition and alloy chromium content (at least in Ni alloys for the range 25-50 wt. % Cr), slightly greater for Ni alloys compared with the Co alloys, and considerably lower than the corresponding rates for pure Cr.

Examination of the scales showed no apparent differences in grain morphology to those formed on pure Cr, no detectable Ni or Co contents (by EPMA) but then this was expected since the effective ambient oxygen pressure was either below or only slightly above the dissociation pressure of NiO or CoO, and perhaps slightly less tendency to spall on cooling.

#### DISCUSSION AND CONCLUSIONS

Based on the present observations and data available in the literature, it is now possible to formulate a growth model for  $\text{Cr}_2\text{O}_3$ . The present measurements provide strong support for the recent suggestion by Lillerud and Kofstad (1).

Firstly, the parabolic growth constant is virtually independent of oxygen fugacity. According to the abbreviated version of Wagner's parabolic equation (8), if  $\text{Cr}_2\text{O}_3$  grows by bulk diffusion of interstitial Cr ions of effective charge  $\alpha$ , then

$$K_p [(\text{oxide thickness})^2/\text{time}] = (\alpha + 1) D_{\text{Cr}}^{\circ} \left\{ (P_{\text{O}_2}^i)^{-\frac{3}{4(\alpha+1)}} - (P_{\text{O}_2}^a)^{-\frac{3}{4(\alpha+1)}} \right\} \quad [1]$$

where  $K_p$  is the parabolic rate constant in terms of oxide thickness,  $D_{\text{Cr}}^{\circ}$  is the self diffusion coefficient of Cr in  $\text{Cr}_2\text{O}_3$  in equilibrium with oxygen at unit activity, and  $P_{\text{O}_2}^i$  and  $P_{\text{O}_2}^a$  are the effective oxygen partial pressures at the inner and outer scale interfaces respectively. In the case of pure Cr,  $P_{\text{O}_2}^i$  is of course the dissociation pressure of  $\text{Cr}_2\text{O}_3$  in contact with Cr, which is  $10^{-21.57}$  atm. at  $1000^\circ\text{C}$ , and hence even at the lowest ambient oxygen poten-

tial used ( $2.4 \times 10^{-10}$  atm)

$$P_{O_2}^a \gg P_{O_2}^i$$

and eqn. [1] reduces to

$$K_p [(\text{oxide thickness})^2 / \text{time}] \simeq (\alpha + 1) D_{Cr}^o (P_{O_2}^i)^{-\frac{3}{4(\alpha + 1)}} \simeq (\alpha + 1) D_{Cr}^i \quad [2]$$

where  $D_{Cr}^i$  is the self diffusion coefficient of Cr in  $Cr_2O_3$  in equilibrium with Cr (i.e. at  $a_{Cr} = 1$ ). Thus, the rate is independent of the external oxygen pressure. Assuming a value of  $\alpha = 3$  (fully ionized interstitials) and converting the measured gravimetric rate constant,  $K_g$ , to  $K_p$

$$K_p = \left(\frac{1}{y\rho_{Ox}}\right)^2 K_g \quad [3]$$

where  $y$  is the average weight fraction of oxygen in the oxide (for  $Cr_2O_3 = \frac{48}{152}$ ) and  $\rho_{Ox}$  is the density of the oxide ( $\rho_{Cr_2O_3} = 5.21 \text{ g/cm}^3$ ), gives an average value of  $D_{Cr}^i$  of  $4.93 \times 10^{-12} \text{ cm}^2/\text{s}$ . This is very close to the value extrapolated (their measurements were in the range 1030-1500°C, so this is only a small extrapolation) from the diffusion experiments of Hagel and Seybolt (6) in hot-pressed compacts of  $Cr_2O_3$ :  $5.57 \times 10^{-12} \text{ cm}^2/\text{s}$ . As referred to earlier, because of the presence of unreacted Cr in the compacts, the effective oxygen potential of the measurements was thought (1) to be equivalent to the dissociation pressure of  $Cr_2O_3$  in contact with Cr.

An alternative view of the growth mechanism would involve Cr transport through the oxide via cation vacancies, when

$$K_p [(\text{oxide thickness})^2 / \text{time}] = (\alpha + 1) D_{Cr}^o \left\{ (P_{O_2}^a)^{\frac{3}{4(1+\alpha)}} - (P_{O_2}^i)^{\frac{3}{4(1+\alpha)}} \right\} \quad [4]$$

Again, with  $P_{O_2}^a \gg P_{O_2}^i$ , the rate constant depends on the  $3/4(1+\alpha)$ th power of the ambient oxygen pressure. This means that over the range of oxygen potentials examined in the present study,  $2.4 \times 10^{-14}$  to  $8.3 \times 10^{-9}$  atm., the rate constant should have increased by a factor of 11 ( $\alpha = 3$ , fully dissociated vacancies) or much greater than that if  $\alpha$  is less than (120 if  $\alpha = 1$ ), and would have been easily detected with the present experimental arrangement.

The dependence of the gravimetric constant  $K_g$  (eqn. [3]) on  $P_{O_2}^a$  for the assumed defect models (eqns. [2] and [4]) along with the experimental values are plotted in Figure 5. Evidently, the data substantiate the interstitial model.

The second piece of evidence presented here is the lower growth constant observed for  $Cr_2O_3$  growth on the alloys. Again, this is a direct consequence of the interstitial model. For alloys, the Cr activity at the alloy/oxide interface is less than unity, and hence, the effective oxygen pressure there is higher than when pure Cr is the substrate. In terms of a vacancy model this would make virtually no difference to the expected growth rate ( $P_{O_2}^a \gg P_{O_2}^i$ ), except at low alloy Cr contents when the diffusion of Cr from the bulk alloy to the scale became rate-controlling (11). Furthermore, this difference in reaction rate, which is approximately an order of magnitude, cannot be accounted for by a variation in oxide grain size. As indicated earlier, no attempts were made for detailed grain size measurements since no significant difference was observable as a function of time or oxygen potential, or between scales formed on pure Cr or the alloys. Nonetheless, based on the grain boundary 'short circuit' model (9, 10), it can be shown that if this were the case, the grain size would have been different by at least an order of magnitude since the 'apparent' rate constant is roughly inversely proportional to the average grain diameter.

As the reaction is diffusion controlled, the Cr concentration (activity) at the alloy/scale interface is uniquely defined and is less than that in the bulk alloy by an amount depending on the ratio of the scale growth constant to the alloy interdiffusion coefficient. In order to estimate this parameter, it is necessary to balance the fluxes of Cr into the scale and from the bulk alloy. Following the usual analysis (11, 12), for the case where the alloy is single-phase, has a concentration-independent interdiffusion coefficient, and where selective oxidation is complete, gives

$$x_{Cr}^i = \frac{x_{Cr}^b - F(\eta)}{1 - F(\eta)} \quad [5]$$

where  $x_{Cr}^i$  and  $x_{Cr}^b$  are the atomic fractions of Cr at the interface and in the bulk alloy, and

$$\eta = \sqrt{\frac{K_c}{2\bar{D}_{all}}} \quad \text{and } F(\eta) = \sqrt{\pi} \exp(-\eta^2) \operatorname{erfc} \eta \quad [6]$$

where  $K_c$  is the so-called "corrosion constant", and represents a parabolic rate constant in terms of the displacement of the alloy/oxide interface,  $\Delta x_{metal}$ , due to scale growth as defined by

$$\Delta x_{metal} = \sqrt{2 K_c t} \quad [7]$$

$K_c$  is thus related to the gravimetric rate constant by

$$K_c = \frac{1}{2} K_g \left[ \frac{1}{\rho_{metal}} \frac{1-y}{y} \right]^2 \quad [8]$$

where  $\rho_{metal}$  is the density of the metal substrate and  $y$ , as defined earlier, is the average weight fraction of oxygen in the oxide. [ $y_{Cr_2O_3} = 0.3158$ ].  $\bar{D}_{all}$  is the alloy interdiffusion coefficient.

For the Ni-Cr system, the alloy interdiffusion coefficient is approximately independent of composition in the range 0-40 wt.% Cr (13) and at 1000°C has a value of  $2.2 \times 10^{-11} \text{ cm}^2/\text{sec}$ . Combining this with the measured gravimetric rate constants for  $Cr_2O_3$  growth on Ni-25 and Ni-50% Cr alloy -  $1.54 \times 10^{-11}$  and  $1.79 \times 10^{-11} \text{ g}^2 \text{ cm}^{-4} \text{ sec}^{-1}$  respectively - and using eqns. [5], [6] and [8] give an atomic fraction of Cr at the alloy/scale interface of 0.1 and 0.35 for the two alloys respectively. The 50% Cr alloy actually contains two phases, the  $\gamma$ -Ni solid solution and an  $\alpha_2$  Cr-rich b.c.c. phase. The solubility limit of Cr is approximately 44% at this temperature. However, this would not significantly alter the calculated Cr-content at the interface.

The effective  $P_{O_2}$  at the alloy scale interface is now obtained by consi-

dering the equilibrium relationship between  $\text{Cr}_2\text{O}_3$  and Cr in the alloy. Thus,

$$p_{\text{O}_2}^i = \frac{1}{(a_{\text{Cr}}^i)^{4/3}} \exp \left[ -\frac{2\Delta G_{\text{Cr}_2\text{O}_3}^\circ}{3RT} \right] \quad [9]$$

where  $\Delta G_{\text{Cr}_2\text{O}_3}^\circ$  is the Gibbs standard free energy of formation of  $\text{Cr}_2\text{O}_3$  and  $a_{\text{Cr}}^i$  the activity of Cr at the alloy/scale interface. On pure Cr,  $a_{\text{Cr}}^i = 1$  and  $p_{\text{O}_2}^i = \pi_{\text{Cr}_2\text{O}_3}$ , the dissociation pressure of  $\text{Cr}_2\text{O}_3$  in contact with pure Cr.

Thus, combining eqns. [2] and [9], the ratio  $\psi$ , of parabolic growth constants for  $\text{Cr}_2\text{O}_3$  on an alloy to that on pure Cr is given by

$$\psi = (a_{\text{Cr}}^i)^{1/\alpha+1} \quad [10]$$

for the case where interstitials are the major defect.

This result is in contrast to that if vacancies were the dominant diffusion species, when  $\psi$  is given by a combination of eqns. [4] and [9]:

$$\psi = \frac{1 - (a_{\text{Cr}}^i)^{-1/\alpha+1} (\pi_{\text{Cr}_2\text{O}_3}/p_{\text{O}_2}^a)^{3/4(1+\alpha)}}{1 - (\pi_{\text{Cr}_2\text{O}_3}/p_{\text{O}_2}^a)^{3/4(1+\alpha)}} \quad [11]$$

In the present case, since  $p_{\text{O}_2}^a \gg \pi_{\text{Cr}_2\text{O}_3}$ , and unless  $a_{\text{Cr}}^i$  is very small,  $\psi$  is little different from unity.

Thus, it is argued that since experimentally,  $\psi \approx 0.15$ , and although this is not entirely consistent with eqn. [10], that fact that is considerably less than unity favors the interstitial model.

Similar calculations for the Co-Cr system, in which  $\tilde{D}_{\text{a11}}$  appears (14-16) to fall in the range  $(3.3-5.5) \times 10^{-12}$   $\text{cm}^2/\text{sec}$ . suggest that  $a_{\text{Cr}}^i$  is somewhat smaller than in the Ni-Cr system. However, diffusion coefficients (Cr tracer in Co-21 wt.% Cr - 2 vol.%  $\text{y}_2\text{O}_3$  (17)) as high as  $10^{-11}$   $\text{cm}^2/\text{sec}$ . have been measured, and this would give Cr concentration at the interface of similar magnitudes to those in the Ni-Cr system. Again, the measured ratio of growth

constants is  $\sim 0.12$ , and there is no evidence that the oxide growth rate is being controlled by Cr diffusion in the underlying alloy, for example a tendency to develop a non-planar alloy/scale interface.

Although the growth constants for  $\text{Cr}_2\text{O}_3$  on the alloys are not quantitatively consistent, they do qualitatively agree with the general behavior observed at higher oxygen potentials (1 atm.): parabolic rate constants for  $\text{Cr}_2\text{O}_3$  growth on Fe, Ni and Co-Cr all increase with increasing alloy Cr content (18). However, under these conditions, it has usually been speculated that this is related to a decrease in the noble metal (Fe, Ni or Co) content of the oxide modifying the defect concentrations. With the present experiments, significant solubility of Ni or Co in the  $\text{Cr}_2\text{O}_3$  is not anticipated since the  $P_{\text{O}_2}$  is either below, or only slightly above the dissociation pressures of NiO or CoO. Nevertheless, the apparent independence of the growth constant on the alloy Cr content, and by implication the content at the alloy/scale interface, is puzzling.

#### ACKNOWLEDGEMENTS

This work was supported by the Director, Office of Energy Research, Office of Basic Energy Sciences, Materials Sciences Division of the U.S. Department of Energy under Contract No. DE-AC03-76SF00098.

#### REFERENCES

1. K. P. Lillerud and P. Kofstad, This journal 127, 2397, 2410 (1980).
2. D. P. Whittle and H. Hindam, Proc. of NACE Conf. on "Corrosion/Erosion of Coal Conversion System Materials," Berkeley, CA. (1982).
3. D. Caplan, A. Harvey and M. Cohen, Corros. Sci. 3, 161 (1963).
4. D. Caplan and G. I. Sproule, Oxid. Met. 9, 459 (1975).
5. F. A. Kröger, Proc. of NACE Conf. on High Temperature Corrosion, San Diego, CA., March (1981).
6. W. C. Hagel and A. U. Seybolt, This journal, 108, 1146 (1961).

7. H. Hindam and D. P. Whittle, to be published.
8. P. Kofstad, "High Temperature Oxidation of Metals", Wiley, New York (1966).
9. J. M. Perrow, W. W. Smeltzer and R. K. Ham, Acta Met. 15, 577 (1967).
10. J. M. Perrow, W. W. Smeltzer and J. D. Embury, Acta Met. 16, 1209 (1968).
11. C. Wagner, This journal 99, 369 (1952).
12. B. D. Bastow, D. P. Whittle and G. C. Wood, Oxid. Met. 12, 413 (1978).
13. Y. E. Ugaste, Fiz. Metal. Metallored. 24, 442 (1967).
14. J. W. Weeton, Trans. ASM 44, 436 (1952).
15. A. Davin, V. Leroy, D. Coutsouradis and L. Habraken, Cobalt 14, 51 (1963).
16. A. Green, D. P. Whittle, J. Stringer and N. Swindells, Scripta Met. 7, 1079 (1973).
17. M. S. Seltzer and B. A. Wilcox, Met. Trans.
18. G. C. Wood, I. G. Wright, T. Hodgkiess and D. P. Whittle, Werk, u. Korr. 21, 900 (1970).

FIGURE CAPTIONS

- Figure 1. Parabolic growth kinetics of  $\text{Cr}_2\text{O}_3$  on pure Cr at  $1000^\circ\text{C}$  in  $\text{CO}_2/\text{CO}$  mixtures.
- Figure 2. Parabolic growth kinetics of  $\text{Cr}_2\text{O}_3$  on pure Cr at  $1000^\circ\text{C}$  in  $\text{CO}_2$ -0.3 vol.% CO at linear gas flow velocities of 0.03, 0.33 and 0.66 cm/sec.
- Figure 3. Fracture section through a spalled flake of  $\text{Cr}_2\text{O}_3$  formed on pure Cr.
- Figure 4. Parabolic growth kinetics for  $\text{Cr}_2\text{O}_3$  on Co-25 Cr and Ni-25 and 50 Cr at  $1000^\circ\text{C}$  in  $\text{CO}_2/\text{CO}$  mixtures.
- Figure 5. Dependence of the gravimetric parabolic rate constant for  $\text{Cr}_2\text{O}_3$  growth on Cr on ambient oxygen potential according to an interstitial (eqn.[2]) and vacancy (eqn.[4]) model, and experimental data.

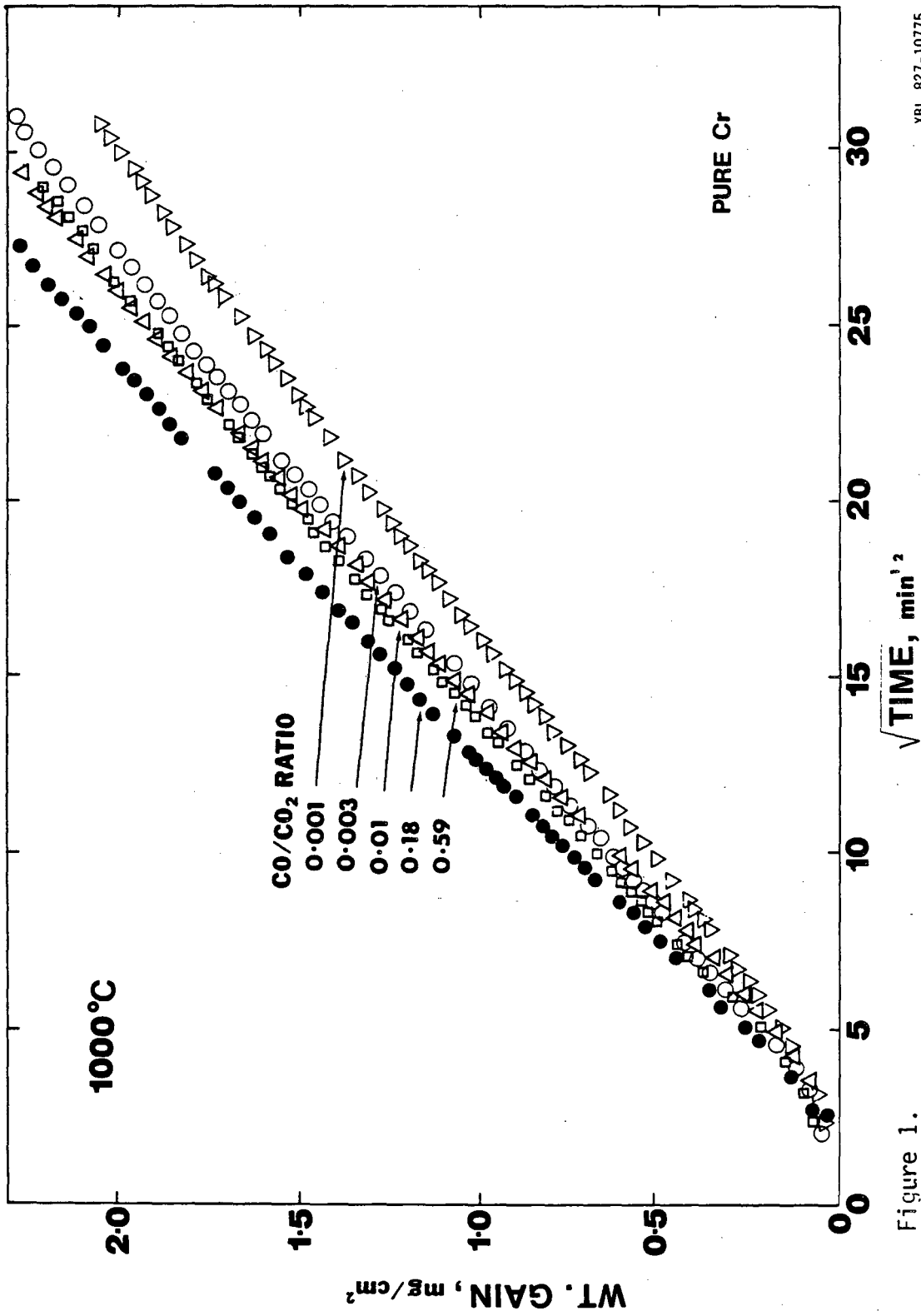


TABLE I. Parabolic Growth Constants for Cr<sub>2</sub>O<sub>3</sub> Growth on Pure Cr at 1000°C.

<u>Gas Mixture</u>	<u>Oxygen Potential, (atm.)</u>	<u>K<sub>g</sub> (g<sup>2</sup> cm<sup>-4</sup> s<sup>-1</sup>)</u>
CO <sub>2</sub> -0.1% CO	8.3 x 10 <sup>-9</sup>	9.21 x 10 <sup>-11</sup>
CO <sub>2</sub> -0.3% CO	9.2 x 10 <sup>-10</sup>	9.50 x 10 <sup>-11</sup>
CO <sub>2</sub> -0.3% CO	9.2 x 10 <sup>-10</sup>	1.00 x 10 <sup>-10</sup>
CO <sub>2</sub> -0.3% CO	9.2 x 10 <sup>-10</sup>	1.07 x 10 <sup>-10</sup>
CO <sub>2</sub> -1% CO	8.2 x 10 <sup>-11</sup>	1.18 x 10 <sup>-10</sup>
CO <sub>2</sub> -15% CO	2.7 x 10 <sup>-13</sup>	1.33 x 10 <sup>-10</sup>
CO <sub>2</sub> -37% CO	2.4 x 10 <sup>-14</sup>	1.03 x 10 <sup>-10</sup>
	mean -----	1.07 x 10 <sup>-10</sup>

TABLE II. Parabolic Growth Constants for Cr<sub>2</sub>O<sub>3</sub> Growth on Alloys at 1000°C.

<u>Alloy</u>	<u>Gas Mixture</u>	<u>Oxygen Potential, (atm)</u>	<u>K<sub>g</sub>(g<sup>2</sup>cm<sup>-4</sup>s<sup>-1</sup>)</u>
Ni-25 wt.% Cr	CO <sub>2</sub> -15% CO	2.7 x 10 <sup>-13</sup>	1.54 x 10 <sup>-11</sup>
Ni-50 wt.% Cr	CO <sub>2</sub> -15% CO	2.7 x 10 <sup>-13</sup>	1.79 x 10 <sup>-11</sup>
Co-25 wt.% Cr	CO <sub>2</sub> -0.1% CO	8.3 x 10 <sup>-9</sup>	1.28 x 10 <sup>-11</sup>
Co-25 wt.% Cr	CO <sub>2</sub> -15% CO	2.7 x 10 <sup>-13</sup>	1.47 x 10 <sup>-11</sup>
Co-25 wt.% Cr	CO <sub>2</sub> -50% CO	8.4 x 10 <sup>-15</sup>	1.15 x 10 <sup>-11</sup>



XBL 827-10775

Figure 1.

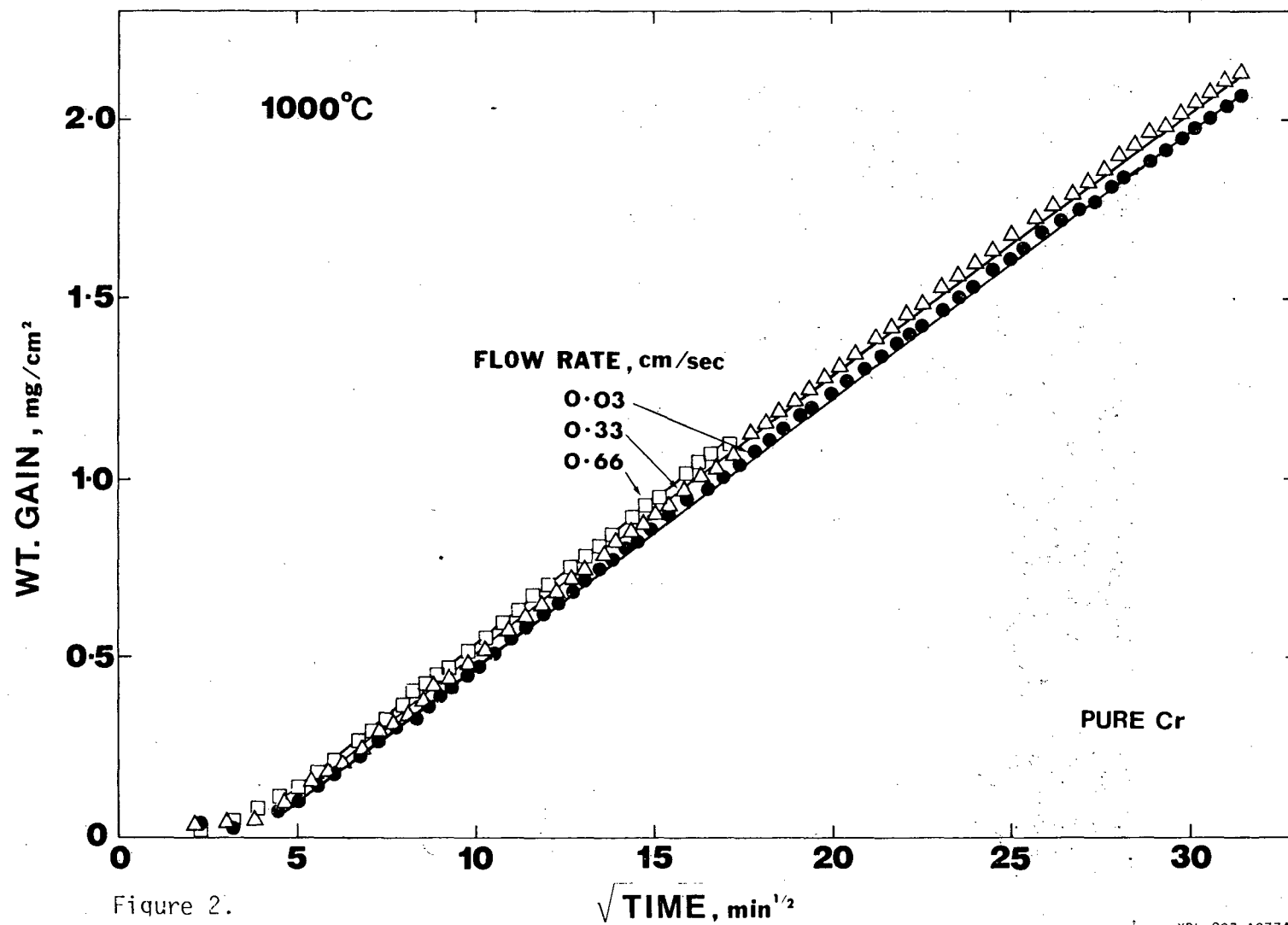


Figure 2.

XBL 827-10774

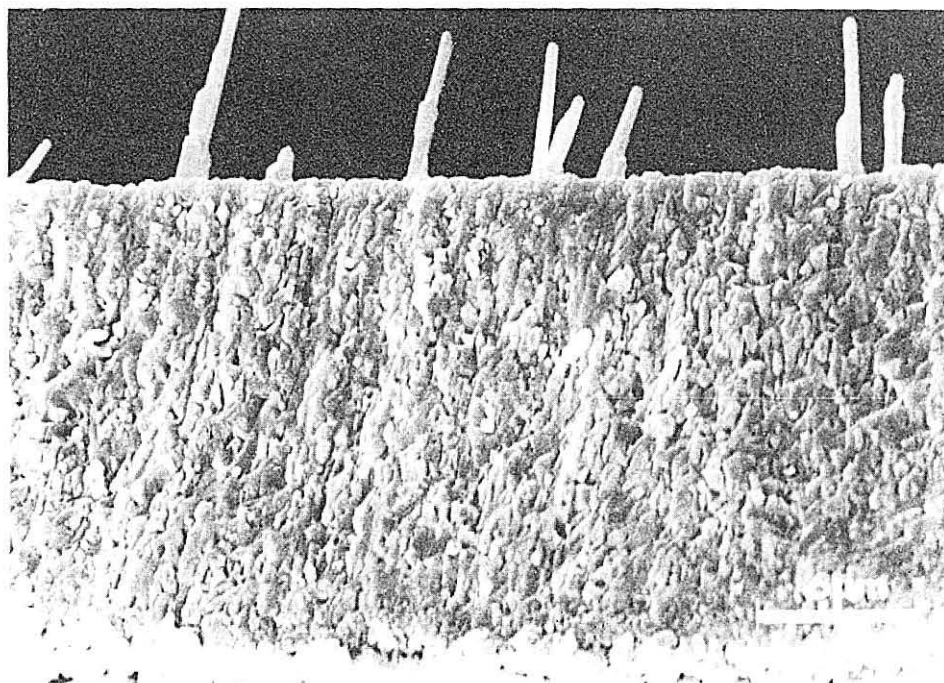


Figure 3.

XBB 827-6260

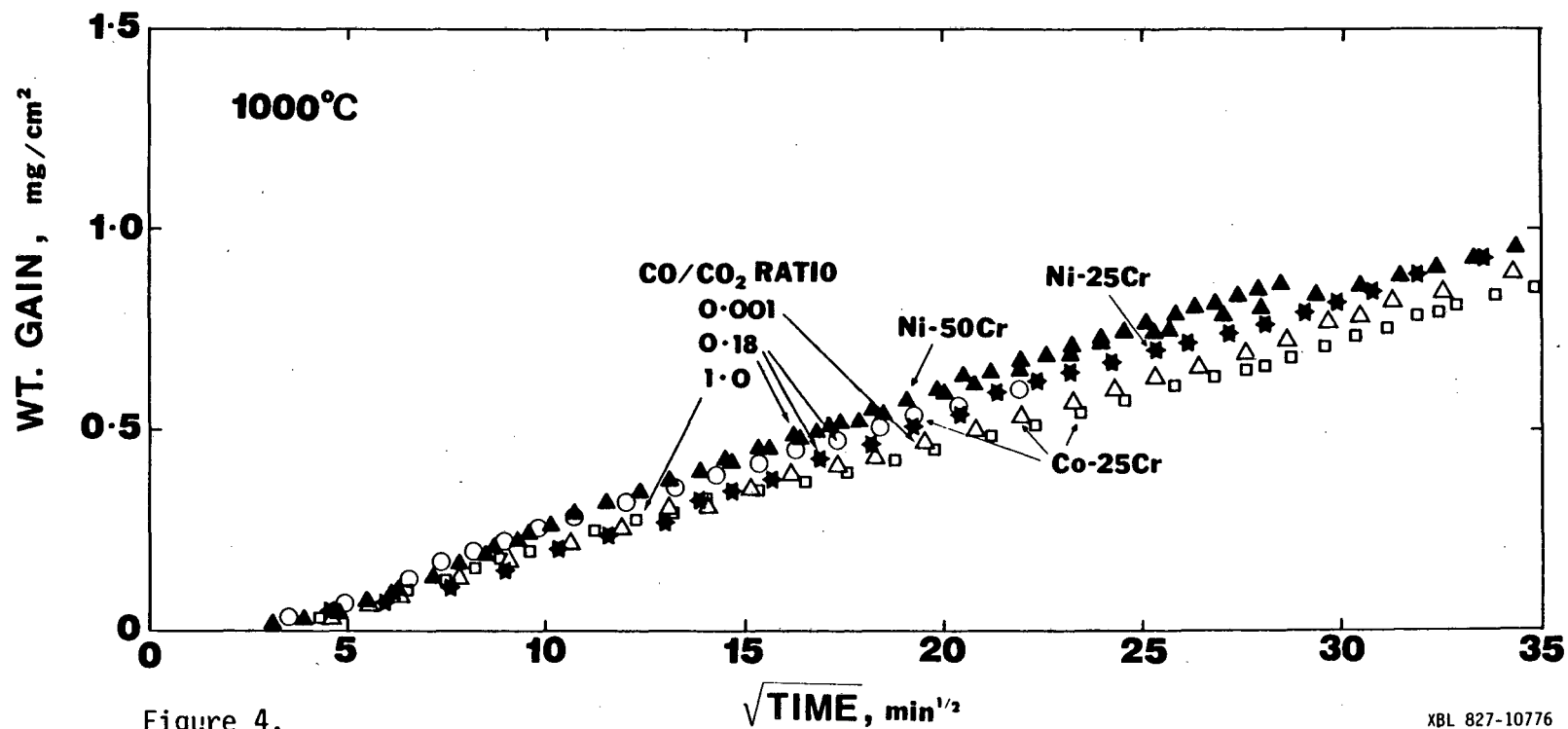


Figure 4.

XBL 827-10776

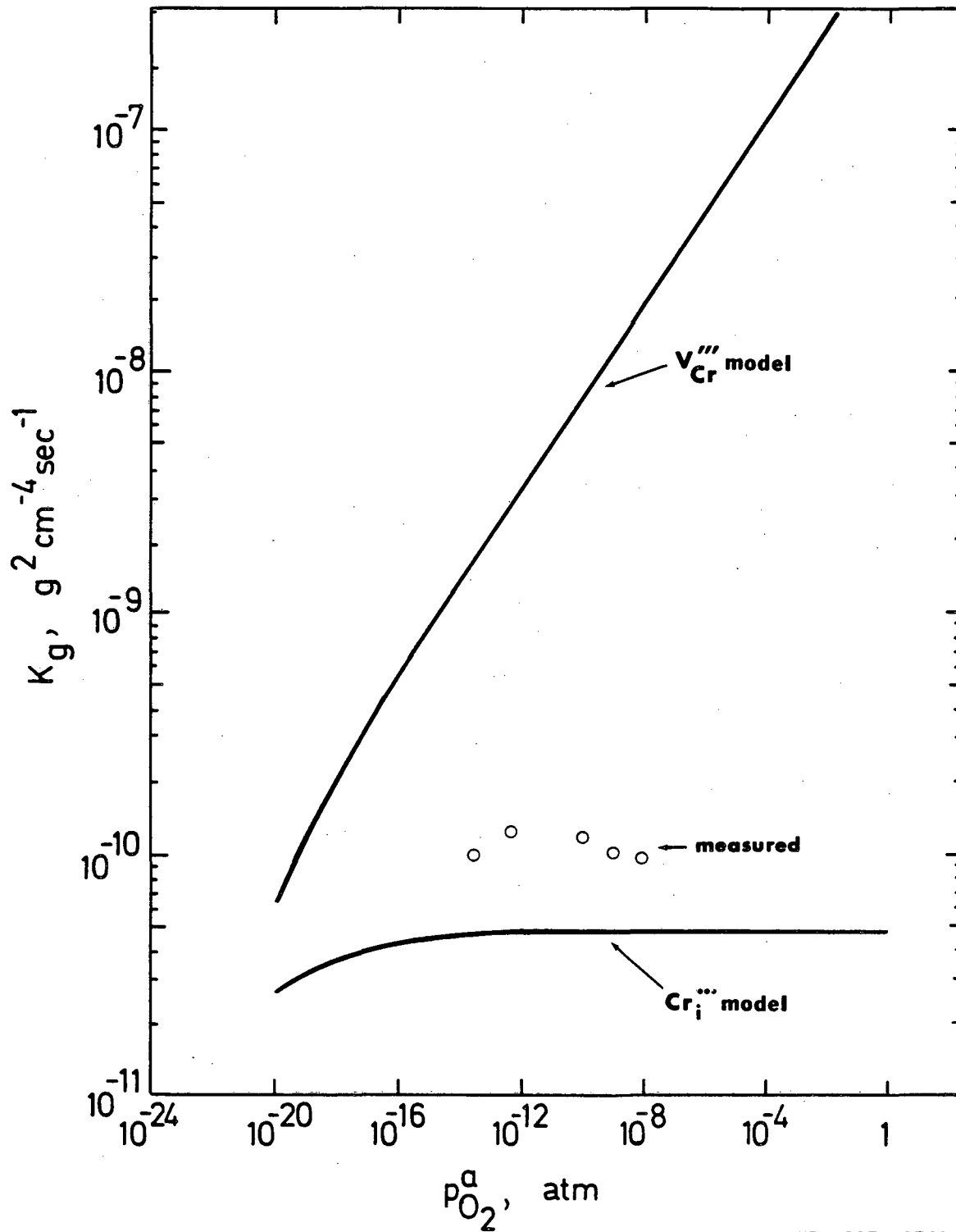


Figure 5.

XBL 827-10769

This report was done with support from the Department of Energy. Any conclusions or opinions expressed in this report represent solely those of the author(s) and not necessarily those of The Regents of the University of California, the Lawrence Berkeley Laboratory or the Department of Energy.

Reference to a company or product name does not imply approval or recommendation of the product by the University of California or the U.S. Department of Energy to the exclusion of others that may be suitable.



TECHNICAL INFORMATION DEPARTMENT  
LAWRENCE BERKELEY LABORATORY  
UNIVERSITY OF CALIFORNIA  
BERKELEY, CALIFORNIA 94720